AgriEngineering

MDPI

Article

Spatiotemporal Dynamics of Land Use and Land Cover through Physical–Hydraulic Indices: Insights in the São Francisco River Transboundary Region, Brazilian Semiarid Area

Lizandra de Barros de Sousa [1,*], Abelardo Antônio de Assunção Montenegro [1], Marcos Vinícius da Silva [1,*], Pabrício Marcos Oliveira Lopes [1], José Raliuson Inácio Silva [1], Thieres George Freire da Silva [1,2], Frederico Abraão Costa Lins [3] and Patrícia Costa Silva [4]

[1] Department of Agriculture Engineering, Federal Rural University of Pernambuco, Street Dom Manoel de Medeiros, Dois Irmãos, Recife 52171-900, PE, Brazil; montenegro.ufrpe@gmail.com (A.A.d.A.M.); pabricio.lopes@ufrpe.br (P.M.O.L.); raliuson.agro@gmail.com (J.R.I.S.); thieres.silva@ufrpe.br (T.G.F.d.S.)
[2] Academic Unit of Serra Talhada, Federal Rural University of Pernambuco, Avenue Gregório Ferraz Nogueira, Serra Talhada 56909-535, PE, Brazil
[3] Center for Higher Education of the São Francisco Valley, BR-315 Highway, Alto do Encanto, Belém do São Francisco 56440-000, PE, Brazil; frederico_acl@hotmail.com
[4] Department of Agricultural Engineering, State University of Goiás, Via Protestato, R. Joaquim José Bueno, Perimetro Urbano, Santa Helena de Goiás 75920-000, GO, Brazil; patricia.costa@ueg.br
* Correspondence: lizandra.barros@ufrpe.br (L.d.B.d.S.); marcos.viniciussilva@ufrpe.br (M.V.d.S.)

Abstract: This article presents a study on the spatiotemporal dynamics of land cover and use, vegetation indices, and water content in the semiarid region of Pernambuco, Brazil. This study is based on an analysis of satellite images from the years 2016, 2018, and 2019 using the MapBiomas platform. The results show changes in the predominant land cover classes over time, with an increase in the caatinga area and a decrease in the pasture area. An analysis of the vegetation indices (NDVI and LAI) indicated low vegetation cover and biomass in the study area, with a slight increase in the NDVI in 2018. An analysis of the Modified Normalized Difference Water Index (MNDWI) showed that the water content in the study area was generally low, with no significant variations over time. An increase in the water bodies, mainly due to the construction of a reservoir, was noted. The results of this study have provided important information for natural resource management in the region, including the development of strategies for the sustainable use and management of natural resources, particularly water resources, vegetation cover, and soil conservation.

Keywords: land cover; land use; vegetation indices; water content; semiarid region

check for updates

Citation: Sousa, L.d.B.d.; Montenegro, A.A.d.A.; Silva, M.V.d.; Lopes, P.M.O.; Silva, J.R.I.; Silva, T.G.F.d.; Lins, F.A.C.; Silva, P.C. Spatiotemporal Dynamics of Land Use and Land Cover through Physical–Hydraulic Indices: Insights in the São Francisco River Transboundary Region, Brazilian Semiarid Area. *AgriEngineering* **2023**, *5*, 1147–1162. https://doi.org/10.3390/agriengineering5030073

Academic Editors: Leonardo Conti, Gabriel Araújo e Silva Ferraz and Giuseppe Rossi

Received: 31 March 2023
Revised: 5 June 2023
Accepted: 23 June 2023
Published: 3 July 2023

Copyright: © 2023 by the authors. Licensee MDPI, Basel, Switzerland. This article is an open access article distributed under the terms and conditions of the Creative Commons Attribution (CC BY) license (https://creativecommons.org/licenses/by/4.0/).

1. Introduction

Semiarid regions, despite being subject to intense rainfall events, have temporally and spatially irregular rains, which cause extreme situations such as droughts and floods [1–4]. In addition, these regions have high evaporation rates and shallow soils with low water retention capacities, which increases water scarcity problems [5–7]. Such characteristics make these regions susceptible to desertification. In the Brazilian semiarid region, there is the only exclusively Brazilian biome, the caatinga, which is predominantly present in the northeast region and has the characteristic of losing its leaves during the dry season, in addition to other attributes that provide the biome with high resistance to drought [4,8,9].

The northeast region is among the areas susceptible to the desertification process, with semiarid and sub-humid climates and subject to intense annual rainfall variations and vegetation suppression [10–14]. Removal of the vegetation cover causes soil erosion, which reduces the water retention capacity and consequently decreases the soil organic matter, leading to soil degradation, threatening biodiversity, and reducing plant biomass [15]. Furthermore, changes in land use and occupation are expected to occur in the semiarid

region of the state of Pernambuco, either due to natural causes related to climate change or induced by the implementation of the São Francisco River Integration Project (PISF), also referred to as the São Francisco River Transboundary Project, with the hydrographic basins of the northern northeast [16,17]. The axes, branches, and pipelines were designed for human and animal water supplies and should also contribute to the expansion of the water supply in Pernambuco [18,19].

The environmental conditions of the semiarid region strongly influence the land use dynamics, as well as biophysical parameters such as the albedo, vegetation, and water indices [20,21]. Environmental monitoring carried out directly in the field is often unfeasible due to operational cost, rainfall seasonality, and the spatial variability of the soil and vegetation characteristics [8]. Thus, the use of remote sensing techniques and a geographic information system (GIS) has been increasingly encouraged for semiarid conditions [22]. The use of remote sensing to obtain data related to land use and the biophysical parameters of the environment in order to conduct studies and monitor natural resources, soil degradation, and vegetation cover has increased in recent years and can assist in the adoption of sustainable practices and management [15,21,23,24].

Studies utilizing very high-resolution land cover data and phenological metrics derived from remote sensing have been instrumental in assessing vegetation status and changes [25–28]. For example, Orusa et al. [25] developed an Earth observation service to map land cover in complex geomorphological areas, enabling continuous mapping with high spatial and temporal resolutions. Another study by Pielke et al. [26] highlighted the impacts of human land management on landscape structure and surface fluxes, emphasizing the need to consider these changes in climate assessments and adaptation strategies. Additionally, Orusa et al. [27] developed an algorithm for mapping phenological metrics in mountain areas worldwide, utilizing high-resolution satellite data to gain insights into land surface phenology and trends.

Biophysical indices (NDVI, LAI, and MNDWI) are available through satellite image processing and have been important input for identifying land cover and land use changes. From temporal analysis of VIs, it is possible to define patterns that characterize a particular culture or group of cultures or even a particular land use dynamic [29]. By monitoring the water behavior associated with vegetation cover variation, it is possible to diagnose anthropogenic and natural alterations in the landscape and guide the establishment of policies to reverse an environmental degradation scenario [30–32]. The Modified Normalized Difference Water Index (MNDWI) developed by Xu [33] has been widely accepted for identifying surface water bodies. This index has proven to be efficient for mapping small reservoirs in hydrographic basins in the semiarid region of Pernambuco [32].

The association of vegetation indices, such as the NDVI and LAI, with such water indices as the MNDWI, using remote sensing techniques and geoprocessing of orbital images, is necessary to assess the intensification of anthropogenic processes. In a study by Silva et al. [34], which evaluated the spatiotemporal changes in environmental degradation processes of vegetation cover and water resources through physical and water-related parameters (NDVI and MNDWI) on the surface, using remote sensing techniques, in northeastern Brazil, the authors observed the impacts of the degradative processes of anthropogenic actions and their intensification on water bodies and vegetation dynamics. Consistently with the aforementioned study, Silva et al. [35], who explored the NDVI, LAI, and MNDWI to characterize natural and anthropogenic degradation processes in a microregion of northeastern Brazil, also emphasized in their study results the importance of applying physical and water indices to highlight soil use and land cover degradation processes. Furthermore, this study addresses the need to fill existing knowledge gaps regarding the environmental and agricultural impacts of the São Francisco River Transboundary Project and some of its associated reservoirs.

Therefore, the present study aims to analyze the land cover and land use changes, vegetation dynamics, and water bodies in a specific region located between the municipalities of Terra Nova and Cabrobó in the state of Pernambuco, Brazil. This study sought to assess

the impacts of agricultural activities and the presence of reservoirs, particularly those associated with the São Francisco River Transboundary Project, on the region's environment. Furthermore, this study examines spatiotemporal variations in vegetation indices such as the Normalized Difference Vegetation Index (NDVI), the Leaf Area Index (LAI), and the Modified Normalized Difference Water Index (MNDWI) to gain insights into vegetation vigor, canopy structure, and water body dynamics. The findings of this study have the potential to contribute significantly to decision-making processes related to natural resource management and conservation in the study area.

2. Materials and Methods

2.1. Characterization of the Study Site

The study area, depicted in Figure 1, is situated between the municipalities of Terra Nova and Cabrobó, within the geographic coordinates of 08°17′38″ S and 39°24′14″ W and of 08°10′29″ S and 39°17′31″ W. It encompasses a total area of 16,481.3 hectares and falls within the São Francisco Mesoregion and the Petrolina Microregion in the state of Pernambuco [36–39]. The study area intersects with the north axis of the São Francisco River Integration Project (PISF), also referred to as the São Francisco River Transboundary Project. The São Francisco River Transboundary Project is a significant water initiative led by the Federal Government of Brazil, spanning a length of 477 km. It comprises two primary axes, the north axis and the east axis, incorporating four tunnels, 14 aqueducts, nine pumping stations, and 27 reservoirs, with 18 of these reservoirs situated in Pernambuco. This project's objective is to secure water supplies for the socio-economic development of drought-prone states such as Ceará, Paraíba, Pernambuco, and Rio Grande do Norte [18,40,41].

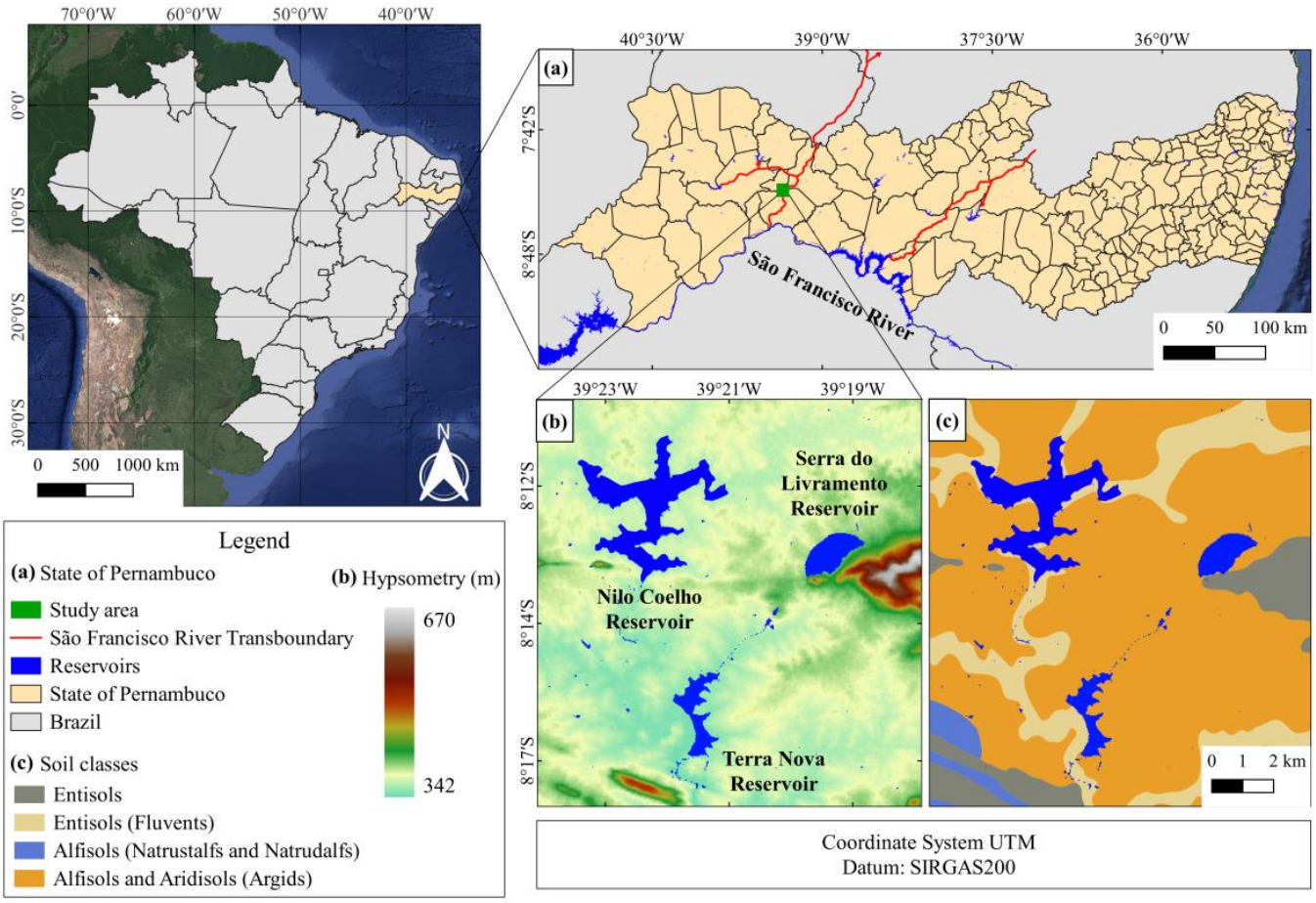

Figure 1. Map of the study area location (**a**), with the elevation (**b**) and soil classes (**c**) of the site.

According to the Köppen–Geiger climate classification, the climate of the region is type BSh (hot, semiarid climate) [42,43], with an average annual rainfall of approximately 600 mm. The wet season begins in January and extends until April [44]. The predominant soil classes are Entisols, Entisols (Fluvents), Alfisols (Natrustalfs and Natrudalfs) and Alfisols and Aridisols (Argids). The vegetation is composed of hyperxerophilic caatinga, with sections of deciduous forests. The relief is predominantly smooth-undulation. Both municipalities are located in the geoenvironmental unit of the Sertaneja Depression and, geologically, in the Borborema Province [36,37,45].

Three main water bodies were identified in the analyzed region. The first is the Nilo Coelho reservoir, located between the municipalities of Terra Nova and Cabrobó. The second and third are the Terra Nova and Serra do Livramento reservoirs, located in Cabrobó, to the north of the municipality. The Nilo Coelho reservoir is used as a water supply source for human consumption and for irrigation use in the municipality, being one of the largest in the Sertão of Pernambuco, with a capacity of 22 million m^3, and was constructed in 1928 [46]. The Terra Nova and Serra do Livramento dams were constructed as part of the north axis of the São Francisco River Transboundary Project, and from the opening of their gates, the waters of the Transboundary Project can be released for human and animal consumption, as well as to increase water supply for irrigation and stream perenization [18,19,47].

2.2. Remote Sensing Data

Three Landsat-8 satellite images were selected; they were acquired from the website https://earthexplorer.usgs.gov/ (accessed on 4 June 2023), an American spatial database of the National Aeronautics and Space Administration/United States Geological Survey (NASA/USGS). The Landsat-8 Operational Land Imager/Thermal Infrared Sensor (OLI/TIRS) is composed of 11 multispectral bands ranging from 0.43 to 12.51 μm in wavelength, with spatial resolutions of 30 m (bands 1 to 9), except for bands 10 and 11, which have spatial resolutions of 100 m; spectral resolutions of 16 bits, representing gray levels from 0 to 65,535; and a temporal resolution of 16 days.

The images used corresponded to the dry period of the region and to the dates of 29 October 2016, 17 September 2018, and 15 October 2019, with orbit 217 and point 66, except for the year 2018, which had orbit 216 and point 66, as shown in Table 1. All images from 2017 for the study area presented clouds; therefore, no analysis was carried out for that year.

Table 1. Image date, time, sun elevation angle, and satellite point.

Date	UTM Time	Sun Elevation Angle	Orbit	Point
29 October 2016	12:48:21	65.9414	217	66
17 September 2018	12:47:38	61.1147	216	66
15 October 2019	12:42:13	65.7611	217	66

Source: USGS [48].

2.3. Rainfall Data

Rainfall data for the years of the imaging dates were analyzed for the study area from 2016 to 2019 using data obtained from the Pernambuco Agency of Water and Climate (APAC)'s Terra Nova weather station and the National Institute of Meteorology (INMET)'s Cabrobó automatic weather station, as shown in Figure 2. The average annual total rainfalls were 490.55 mm (2016), 533.1 mm (2018), and 417.2 mm (2019).

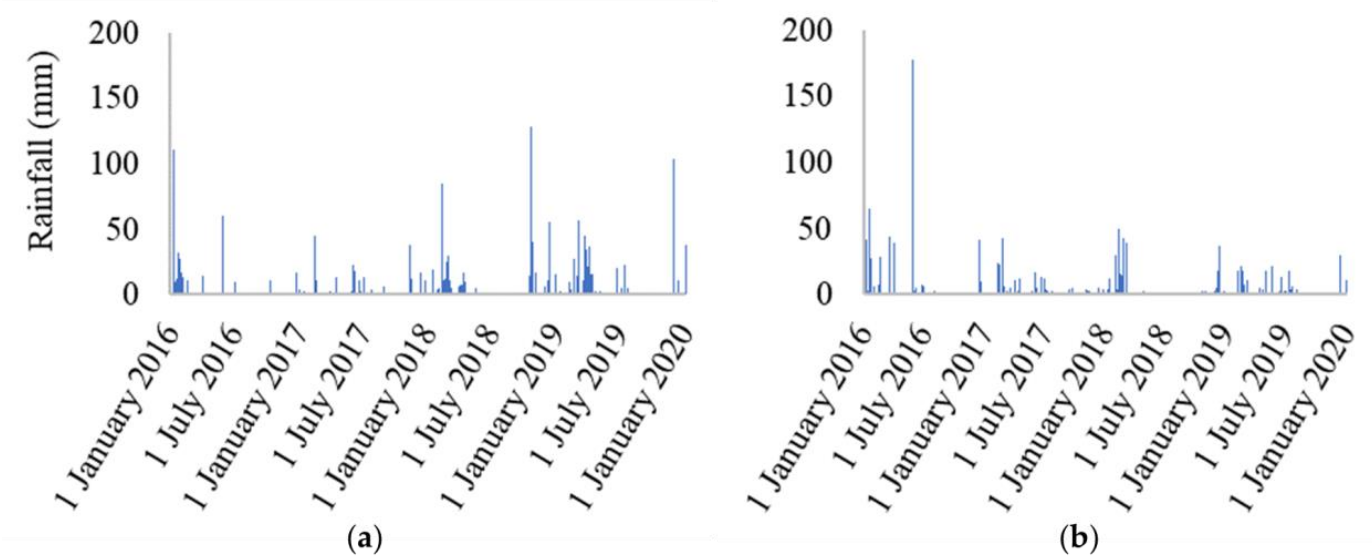

Figure 2. Daily rainfall (mm) from 2016 to 2019 for the (**a**) Terra Nova weather station and (**b**) Cabrobó automatic weather station, Pernambuco. Sources: APAC [49] and INMET [44].

2.4. Land Use and Land Cover Classifications

The land use and land cover classifications for Brazil were based on images freely available on the online platform MapBiomas, which has classifications, available up to 2019, based on Landsat satellite images with spatial resolutions of 30 m. Maps were generated for the years 2016, 2018, and 2019. The classified images were from Collection 5, which uses a catalog with 27 classes [50]. Afterward, the area of the class related to water bodies was calculated to quantify the evolution of these areas over time.

2.5. Calculation of Water and Vegetation Indices

The Normalized Difference Vegetation Index (NDVI) is the most commonly used vegetation index and is an indicator of photosynthetically active biomass. It is calculated as the ratio of the differences between the near-infrared (ρ_{NIR}) and red (ρ_R) bands, respectively to their sums, as shown in Equation (1) [51]:

$$\text{NDVI} = \frac{\rho_{NIR} - \rho_R}{\rho_{NIR} + \rho_R} \quad (1)$$

The Soil-Adjusted Vegetation Index (SAVI) was calculated according to Equation (2), and it is an indicator of the amount and condition of green vegetation that seeks to mitigate the background effects of soil [52]:

$$\text{SAVI} = \frac{(1 + \text{L})(\rho_{NIR} - \rho_R)}{\text{L} + \rho_{NIR} + \rho_R} \quad (2)$$

where ρ_R and ρ_{NIR} are the red and near-infrared bands, respectively, and L is a factor depending on the type of soil, considered to be 0.5 for this study [7,20,53–55].

The Leaf Area Index (LAI) is defined as the ratio of the total leaf area to the area of land used by that vegetation. It is an indicator of the biomass of each pixel of an image, computed with Equation (3) [53]:

$$\text{LAI} = \frac{-\ln\left(\frac{0.69 - \text{SAVI}}{0.59}\right)}{0.91} \quad (3)$$

The Modified Normalized Difference Water Index (MNDWI) was proposed by Xu [33] and aims to highlight water features and identify watercourses. It is calculated as the ratio between the differences of the reflectance values of the visible green (ρ_G) and medium infrared (ρ_{MIR}) bands, divided by their respective sums, as shown in Equation (4). The

MNWDI ranges from −1 to +1, and values above zero are indicative of the presence of water bodies. Subsequently, the delimitation of the water bodies was vectorized and exported and their area calculated.

$$\text{MNDWI} = \frac{\rho_G - \rho_{MIR}}{\rho_G + \rho_{MIR}} \quad (4)$$

2.6. Image Processing and Statistical Analysis

All images were processed in QGIS software version 3.22, and reflective bands from 2 to 7 were used in the Landsat-8 satellite images. To determine the vegetation and water indices, the Semiautomatic Classification Plus (SCP) plugin was used, converting gray levels to radiance and reflectance using radiometric calibration coefficients found in the image metadata. Subsequently, processing was carried out considering the scene cuts according to the areas of interest, and the images were reprojected to SIRGAS2000.

For the visualization of the region, false color composites of bands 5, 4, and 3 (for the Landsat-8 images) were used for the near-infrared, red, and green bands, respectively, as shown in Figure 3.

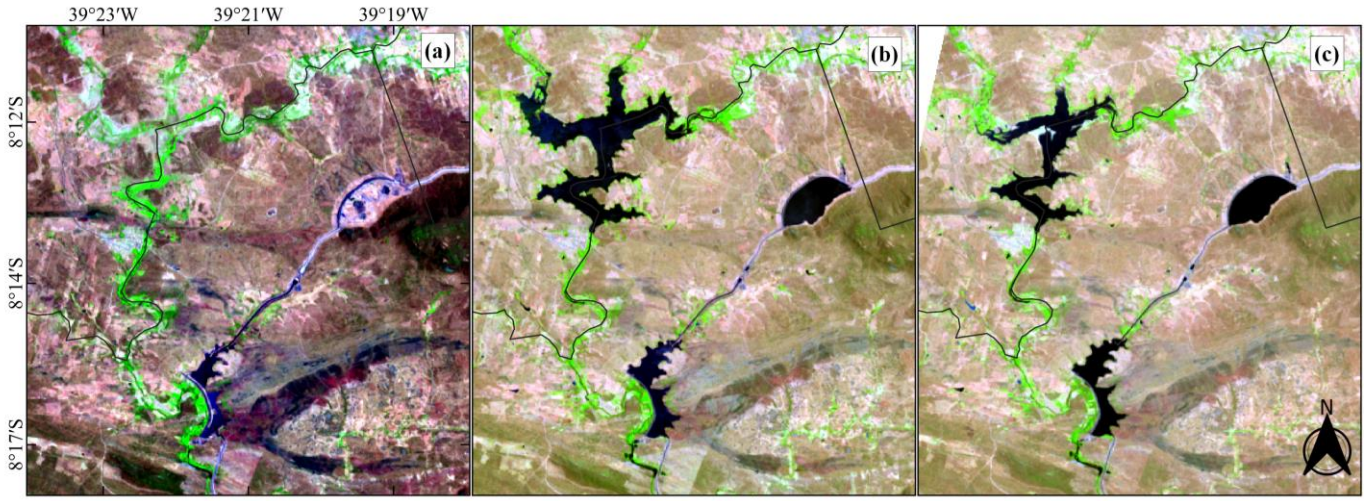

Figure 3. False color compositions of Landsat-8 images for the dates 29 October 2016 (**a**), 17 September 2018 (**b**), and 15 October 2019 (**c**).

The QGIS "Raster Calculator" tool was used to calculate the NDVI, LAI, and MNDWI. Afterward, the values of these indices for all pixels within the region were extracted. These extracted values were then subjected to descriptive statistics, including measures such as the minimum, maximum, mean, standard deviation (SD), and coefficient of variation (CV).

3. Results

The annual thematic classification maps of land cover and use for the study area in the years 2016, 2018, and 2019 were developed based on the MapBiomas platform, which allowed us to infer the main cover classes that make up the site (Figure 4 and Table 2). The year 2016 (Figure 4a) presented coverage percentages of forest, savanna, and grassland formations of 0.04, 43.68, and 20.02%, respectively. In 2018 (Figure 4b), there were increases, with values of 0.10, 44.83, and 23.29%, respectively. Similarly, for 2019 (Figure 4c), the percentages were 0.16, 46.48, and 23.08%, respectively.

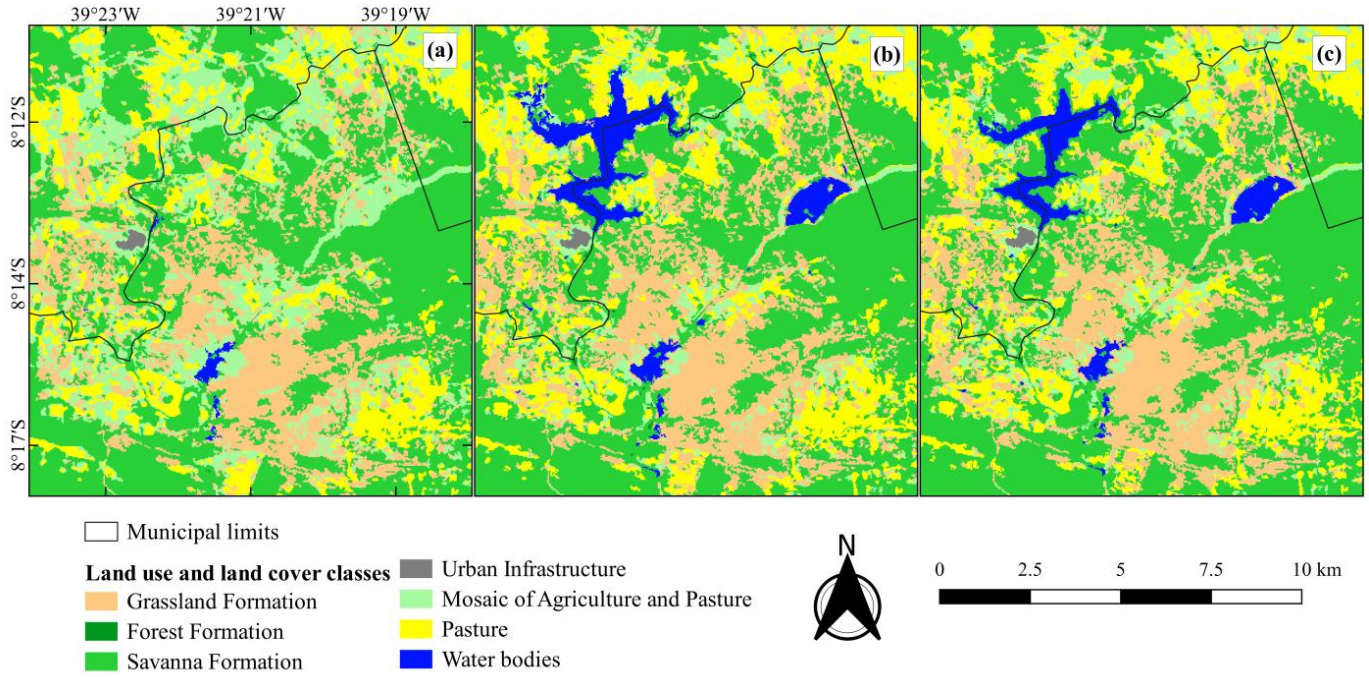

Figure 4. Land use and land cover classifications in the study area for the years 2016 (**a**), 2018 (**b**), and 2019 (**c**).

Thus, the transition from 2016 (Figure 4a) to 2018 (Figure 4b) showed an increase in the caatinga area (forest, savanna, and grassland formations) of 7.00% and a reduction in the agriculture and pasture areas (pastures and agriculture–pasture mosaic) of 23.62%. When 2016 and 2019 were compared (Figure 4c), there were a 9.35% increase in the caatinga area and a 25.38% reduction in the agriculture and pasture areas. This indicates a shift in land use practices and a potential conversion of agricultural and pasture areas into natural vegetation formations.

Table 2. Area (hectares) and percentages (%) of land use and land cover classifications.

Land Use and Land Cover Classification	2016 (ha)	2016 (%)	2018 (ha)	2018 (%)	2019 (ha)	2019 (%)
Forest Formation	7.07	0.04%	15.74	0.10%	25.56	0.16%
Savanna Formation	7053.07	43.68%	7237.80	44.83%	7503.64	46.48%
Grassland Formation	3232.31	20.02%	3759.63	23.29%	3725.85	23.08%
Pasture	2495.44	15.46%	3020.41	18.71%	2974.25	18.42%
Mosaic of Agriculture and Pasture	3269.79	20.25%	1382.94	8.57%	1327.67	8.22%
Urban Infrastructure	29.89	0.19%	30.42	0.19%	30.33	0.19%
Water Bodies	57.92	0.36%	698.56	4.33%	558.21	3.46%

Another factor that changed the landscape was the increase of 1106.08% in the areas covered by water bodies from 2016 to 2018, mainly due to an increase in the volume of the Nilo Coelho reservoir and the completion of the Transboundary axis, which includes the Terra Nova and Serra do Livramento reservoirs. These developments have contributed to increased water availability in the region. It is worth noting that despite being constructed in 1928, the Nilo Coelho reservoir was completely dry in the year 2016 (Figure 4a).

Figure 5 shows the spatiotemporal distributions of the Normalized Difference Vegetation Index (NDVI) for 2016, 2018, and 2019, in the dry season, where the values range from 0 to 0.6. NDVI values between 0 and 0.3 are considered more susceptible to degradation, presenting areas with bare soil and sparse vegetation, according to false-color composition images (Figure 3). The NDVI is an index related to vegetation activity, and the closer it is

to 1, the higher the photosynthesis and transpiration are [56]. When the NDVI is between 0 and 0.30, it indicates the occurrence of herbaceous vegetation or that the caatinga is leafless [57].

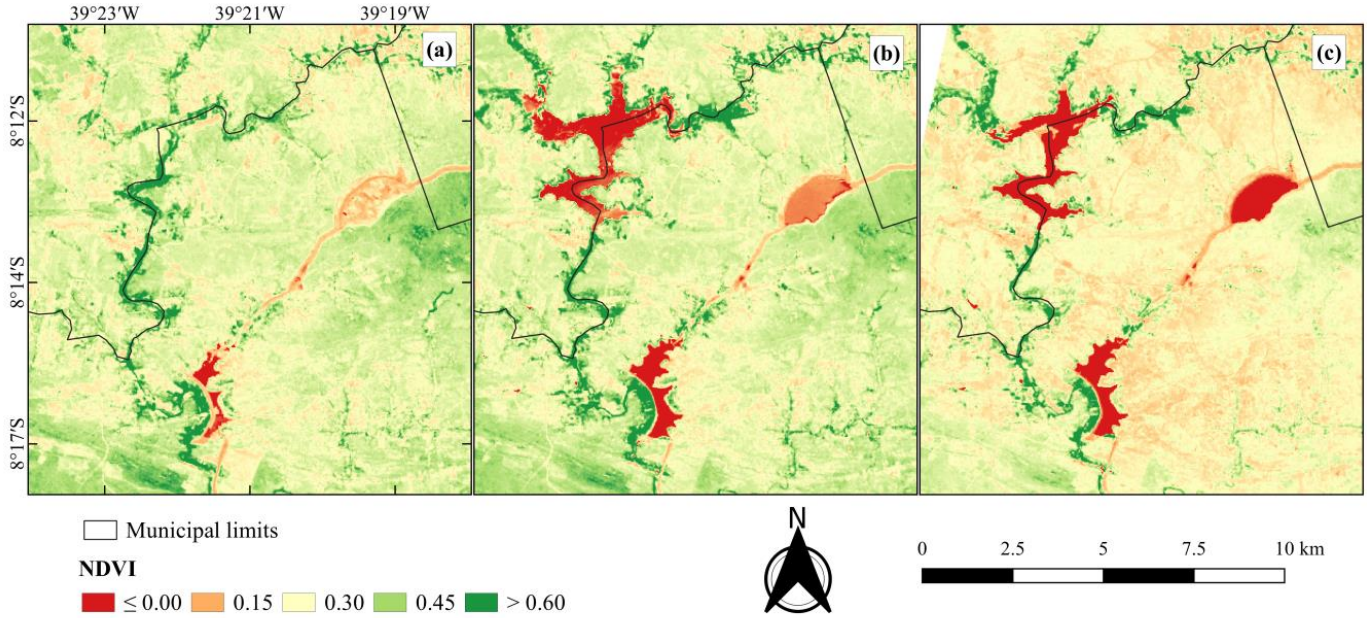

Figure 5. Spatiotemporal distributions of the Normalized Difference Vegetation Index (NDVI) for the dates 29 October 2016 (**a**), 17 September 2018 (**b**), and 15 October 2019 (**c**).

Areas with NDVI values of greater than 0.45 represent regions of high vegetative vigor. Therefore, it can be observed in Figure 5b that these areas are more evident along the reservoir margins and near the drainage network, indicating that the soil moisture is preserved even during the dry season. However, because they have fertile soils and preserve soil moisture for a longer time, the regions close to the drainage networks have their native vegetation constantly removed [32]. The total annual precipitation in 2018 was high, which may have also influenced the result, as in 2019, the total annual precipitation was the lowest compared to other years.

Figure 6 shows the maps of the Leaf Area Index (LAI), which present values ranging from 0 to 0.5 m^2/m^2 for the study area over the analyzed period; lower values of the LAI correspond to lower values of the Soil Adjusted Vegetation Index (SAVI). The distribution of the LAI is similar to the distribution of the NDVI; however, the LAI is a parameter that is related to the structure of the canopy, consequently affecting rain interception, light interception, and gas exchange [58]. Additionally, it is worth noting that the caatinga vegetation is highly dynamic, with accelerated growth during the wet season and leaf loss during the dry season [56]. The satellite images used in the present study were obtained during dry months; consequently, we found low LAI values due to the native vegetation losing its leaves.

Figure 7 shows the spatiotemporal distributions of the Modified Normalized Difference Water Index (MNDWI) for 2016, 2018, and 2019, where the values range from 0 to −1.0. This index minimizes information about vegetation and highlights water bodies (reservoirs, lakes, dams, and rivers) [33].

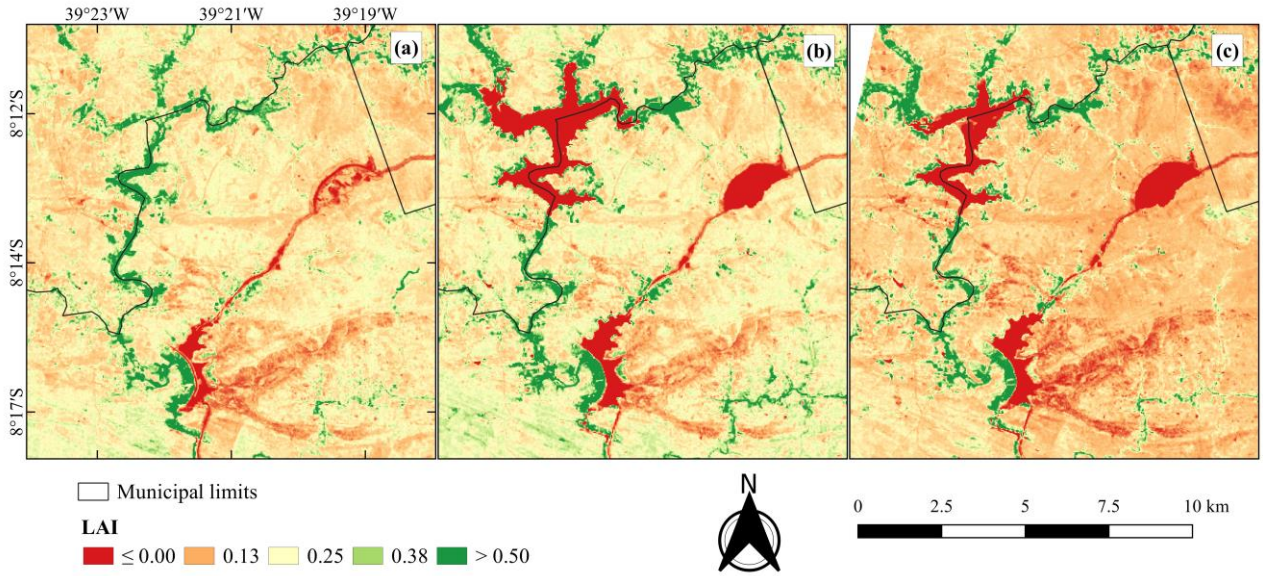

Figure 6. Spatiotemporal distributions of Leaf Area Index (LAI) for the dates 29 October 2016 (**a**), 17 September 2018 (**b**), and 15 October 2019 (**c**).

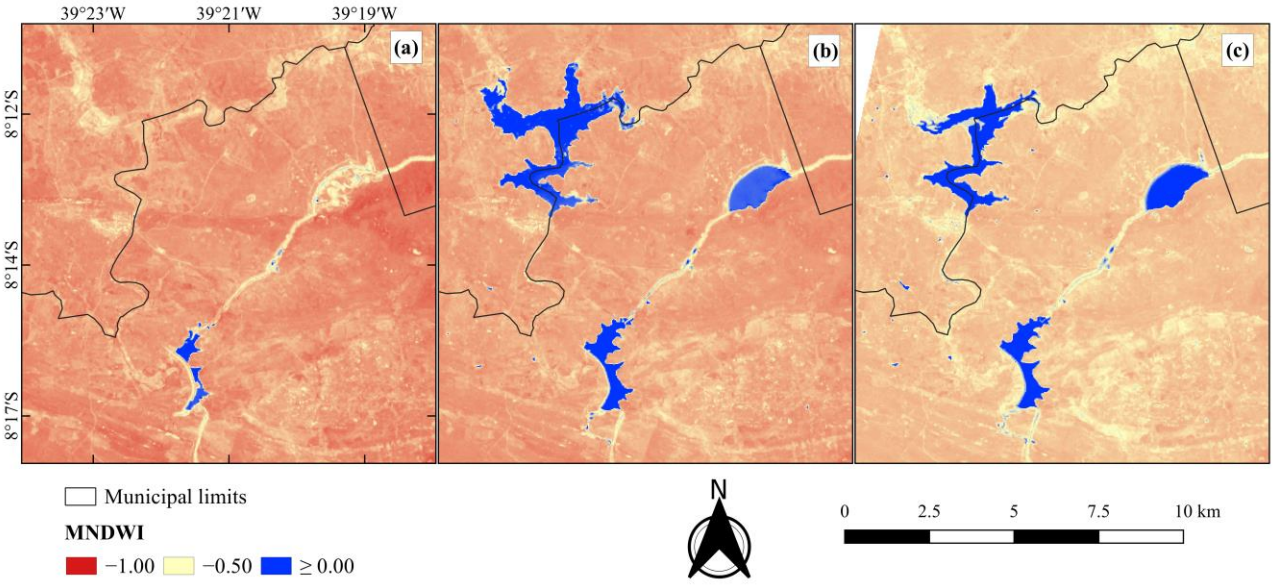

Figure 7. Spatiotemporal distributions of the Modified Normalized Difference Water Index (MNDWI) for the dates 29 October 2016 (**a**), 17 September 2018 (**b**), and 15 October 2019 (**c**).

Figure 8 shows the respective surface areas of the reservoirs, determined through land use classification using the MapBiomas product and also through geoprocessing. For this, it was necessary to vectorize the regions corresponding to the water features extracted from the MNDWI on the dates of 29 October 2016, 17 September 2018, and 15 October 2019, shown in blue tones in Figure 7. Using the automated classification acquired with MapBiomas Collection 5, it was possible to observe similarities with the visual interpretation that the MNDWI maps demonstrated regarding the water bodies in the study area. As depicted in Figure 4, the image classifications for those years displayed similarities in the configurations of the water body surface area. The differences between the MNDWI and MapBiomas are related to the Landsat 8 image dates not coinciding with MapBiomas and to how the MNDWI has the potential to identify small reservoirs [59] that contribute to a larger total area of water bodies.

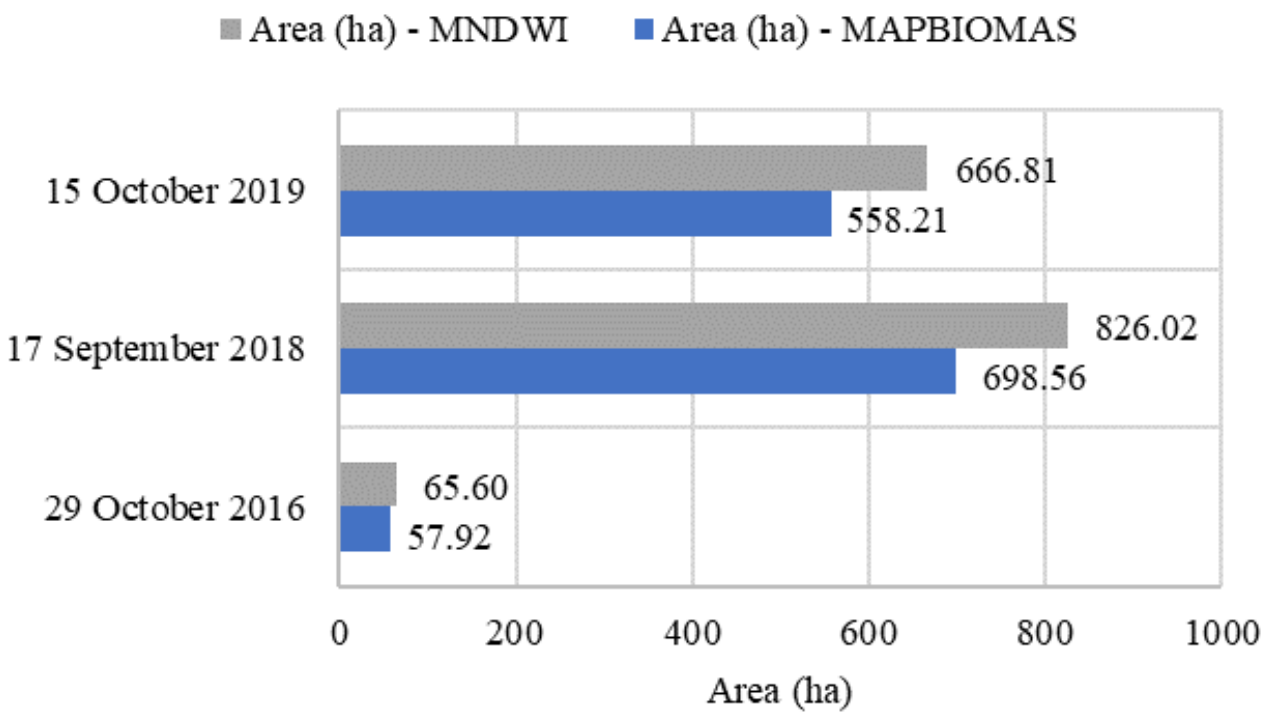

Figure 8. Surface areas of the reservoirs in the years 2016, 2018, and 2019.

For a statistical analysis of the collected data, Table 3 presents the minimum, maximum, mean, standard deviation, and coefficient-of-variation values for each year. It is evident that the NDVI mean on 29 October 2016 (0.356) was higher compared to those on 17 September 2018 (0.344) and 15 October 2019 (0.288). The NDVI values serve as an indicator of vegetation vigor in the study area. The higher NDVI mean in 2016 suggests a healthier vegetation state during that period. However, subsequent years exhibited a decrease in the mean NDVI, indicating a potential decline in vegetation vigor. Several factors could contribute to this decline, including drought conditions or changes in land use, such as the construction of two reservoirs in the study area.

Table 3. Statistical data of the NDVI, LAI, and MNDWI.

Date	Minimum	Maximum	Mean	SD [1]	CV [2] (%)
			NDVI		
29 October 2016	−0.483	0.953	0.356	0.086	24.22%
17 September 2018	−0.591	0.919	0.344	0.118	34.38%
15 October 2019	−0.684	0.870	0.288	0.121	42.09%
			LAI		
29 October 2016	−0.377	5.800	0.237	0.145	60.95%
17 September 2018	−0.362	4.860	0.241	0.184	76.33%
15 October 2019	−0.380	6.330	0.190	0.170	89.65%
			MNDWI		
29 October 2016	−0.902	0.492	−0.708	0.068	9.56%
17 September 2018	−0.862	0.567	−0.645	0.169	26.23%
15 October 2019	−0.734	0.641	−0.581	0.168	28.97%

[1] SD = standard deviation, [2] CV = coefficient of variation.

The MNDWI values provide valuable insights into the presence of water bodies, with negative values close to zero indicating the presence of water. It is evident that in 2019 (−0.581), the negative MNDWI values were more prominent compared to in 2016

(−0.708) and 2018 (−0.645), suggesting a higher occurrence of water bodies during that period. Furthermore, the coefficient of variation (CV) values serve as an indicator of data heterogeneity or variability. In 2019, both the NDVI (42.09%) and the MNDWI (28.97%) exhibited higher CV values compared to those of 2016 and 2018. This indicates that the data for 2019 displayed greater heterogeneity, suggesting more diverse responses of vegetation and water bodies to environmental conditions.

This increased heterogeneity in 2019 could potentially be attributed to factors such as elevated rainfall or changes in water management practices in the region, such as the implementation of the Transboundary Project. The presence of water bodies plays crucial roles in sustaining vegetation and preserving soil moisture, particularly in arid or semiarid regions like the study area. The high dispersion observed in the vegetation indices can be attributed to the various types of soil cover present in the study area, with seven distinct types identified.

4. Discussion

The results of this study suggest that there were changes in the land cover and use in the study area between the time periods of 2016–2018 and 2016–2019, including an increase in the caatinga area and reductions in agriculture and pastures. The increase in the native vegetation areas may be related to the severe drought that occurred in the region between the years 2012 and 2015; in view of these scenarios, several farmers reduced or abandoned agricultural activities, favoring the natural regeneration process of native vegetation [60]. Similar results were obtained by Silva et al. [8] in the transition between 2017 and 2018, when they studied changes caused by agricultural activity in a semiarid region with a predominant caatinga biome in a historical series from 1998 to 2018, with orbital images from Landsat-5 and Landsat-8 satellites. They found that an increase in agriculture resulted in the degradation of the caatinga biome areas and that the recession of livestock farming promoted the natural recovery of the biome.

These results also highlight the importance of reservoirs in the socio-economic development of the region, as they enable irrigation of small areas, guarantee water for livestock and human consumption, and contribute to the recharge of underground aquifers and reductions in potential flash floods [61]. Bi et al. [62] emphasized that the MNDWI is efficient for identifying water reservoirs. We could see that this method identified more reservoirs with smaller water surfaces than did the survey carried out with MapBiomas (Figure 3).

The spatiotemporal distributions of the NDVI, LAI, and MNDWI in the study area provided valuable information about the vegetation vigor, canopy structure, and water bodies. The caatinga biome, where the study area is located, experiences distinct wet and dry seasons, which significantly impacts vegetation dynamics. This natural variability in weather patterns, characterized by periods of rainfall followed by drought, may explain the observed variations in the vegetation indices across different years [56].

Additionally, it is important to consider the influence of the construction of two reservoirs in the study area through the São Francisco River Transboundary Project. The presence of these reservoirs can modify the local water availability and potentially affect the distribution of water bodies, leading to changes in the MNDWI values and influencing the overall vegetation dynamics in the area. Therefore, the combination of climatic factors and human interventions such as the Transboundary Project contributed to the observed variations in the vegetation indices. Sousa et al. [63], in their study of the Terra Nova River Basin, found that there was a direct influence of the release of water from the Terra Nova reservoir of the Transboundary Project on an increase in vegetation cover and expansion of crops along the riverside region. Persistent water features along non-perennial rivers are important resources, providing habitats for plants, animals, and humans during dry periods. These features, which include pools, springs, waterholes, and wetlands, can be sustained by aquifers or runoff [64]. The presence of persistent water along rivers that are typically seasonal is common in different climatic zones around the world, and in

Brazil, it is especially used in semiarid regions for artificial perpetuation of rivers through construction of water reservoirs. These human works alter the natural dynamics of water systems, generating anthropic hydrographic basins [65,66].

One of the limitations of our study is that is that this analysis was based on Landsat-8 satellite images, which have spatial resolutions of 30 m. Although these are high-resolution images, using very-high-resolution imagery could provide more detailed information on land cover and land use changes. It is worth noting that very-high-resolution Earth observation data are currently not available in an open-source format for all users [27]. Despite this, important results are being obtained from high-resolution images in the Brazilian semiarid region [4,8,9,35,63,67]. For instance, a study by Sousa et al. [67] on the spatial distribution of the annual precipitation in a Brazilian semiarid basin and its impact on land use and land cover dynamics (vegetation–water nexus) used images with resolutions of 30 m, thus providing information on rainfall patterns and their correlation with vegetation and water availability.

Regarding future research and studies on land cover and land use changes, vegetation dynamics, and water bodies in the semiarid region, it would be interesting to apply this methodology to all areas affected by the São Francisco River Transboundary Project and assess the positive and negative impacts of this endeavor on the region. Another alternative is cloud processing, such as developing scripts in Google Earth Engine (GEE) to analyze the spatial and temporal variabilities of vegetation vigor, canopy structure, and water body dynamics. This can help identify landscapes where intensification of anthropogenic processes is occurring.

Overall, the results of this study have provided valuable information about land cover and use changes, vegetation activity, and water bodies in the study area, which can be used to support decision-making processes related to natural resource management and conservation.

5. Conclusions

In this study, we aimed to analyze the land cover and land use changes, vegetation dynamics, and water bodies in a specific region located between the municipalities of Terra Nova and Cabrobó in the state of Pernambuco, Brazil. Our findings have important implications for understanding the impacts of agricultural activities and the presence of reservoirs, particularly those associated with the São Francisco River Transboundary Project, on the region's environment. Additionally, we examined the spatiotemporal variations in such vegetation indices as the Normalized Difference Vegetation Index (NDVI), the Leaf Area Index (LAI), and the Modified Normalized Difference Water Index (MNDWI) to gain insights into vegetation vigor, canopy structure, and water body dynamics.

Based on our analysis, we observed significant changes in land cover and land use in the study area over the analyzed period. The expansion of agricultural activities and the construction of reservoirs associated with the São Francisco River Transboundary Project have led to changes in vegetation patterns and the dynamics of water bodies. These changes have important implications for the environment and the sustainability of the natural resources in the region.

The results of our study highlight the importance of utilizing remote sensing techniques and geoprocessing of orbital images for monitoring and assessing of environmental changes in semiarid regions. The use of biophysical indices, such as the NDVI, LAI, and MNDWI, provides valuable insights into the intensification of anthropogenic processes and can guide the development of policies and management strategies to mitigate environmental degradation.

In conclusion, this study contributes to the understanding of land cover and land use changes, vegetation dynamics, and water body dynamics in the semiarid region of Pernambuco, Brazil. These findings have implications for sustainable natural resource management and conservation in the study area. Further research is needed to expand this analysis to other regions and to incorporate very-high-resolution imagery for more-detailed assessments.

Author Contributions: Conceptualization, L.d.B.d.S.; methodology, L.d.B.d.S., P.M.O.L., M.V.d.S. and J.R.I.S.; software, L.d.B.d.S. and F.A.C.L.; validation, L.d.B.d.S.; investigation, L.d.B.d.S. and M.V.d.S.; resources, L.d.B.d.S. and M.V.d.S.; data curation, L.d.B.d.S. and J.R.I.S.; writing—original draft preparation, L.d.B.d.S.; writing—review and editing, A.A.d.A.M., M.V.d.S., L.d.B.d.S., J.R.I.S., F.A.C.L., P.C.S. and T.G.F.d.S.; visualization, A.A.d.A.M., P.M.O.L. and T.G.F.d.S.; supervision, L.d.B.d.S. and P.M.O.L.; project administration, L.d.B.d.S. and P.M.O.L.; funding acquisition, A.A.d.A.M. All authors have read and agreed to the published version of the manuscript.

Funding: This research received no external funding.

Institutional Review Board Statement: Not applicable.

Informed Consent Statement: Not applicable.

Data Availability Statement: Not applicable.

Acknowledgments: We acknowledge the Postgraduate Program in Agricultural Engineering (PGEA) of the Federal Rural University of Pernambuco (UFRPE) for supporting the development of this research and the Coordination of Superior Level Staff Improvement (CAPES), the Foundation for the Support of Science and Technology of the State of Pernambuco (FACEPE—APQ-0300-5.03/17 and IBPG-0855-5.03/20), and the National Council for Scientific and Technological Development (CNPq—140281/2022-3) for the incentive of research scholarships.

Conflicts of Interest: The authors declare no conflict of interest.

References

1. Hu, J.; Yang, Z.; Hou, C.; Ouyang, W. Compound Risk Dynamics of Drought by Extreme Precipitation and Temperature Events in a Semi-Arid Watershed. *Atmos. Res.* **2023**, *281*, 106474. [CrossRef]
2. Dong, T.; Liu, J.; Liu, D.; He, P.; Li, Z.; Shi, M.; Xu, J. Spatiotemporal Variability Characteristics of Extreme Climate Events in Xinjiang during 1960–2019. *Environ. Sci. Pollut. Res.* **2023**, *30*, 57316–57330. [CrossRef]
3. de Brito, C.S.; da Silva, R.M.; Santos, C.A.G.; Brasil Neto, R.M.; Coelho, V.H.R. Monitoring Meteorological Drought in a Semiarid Region Using Two Long-Term Satellite-Estimated Rainfall Datasets: A Case Study of the Piranhas River Basin, Northeastern Brazil. *Atmos. Res.* **2021**, *250*, 105380. [CrossRef]
4. Refati, D.C.; da Silva, J.L.B.; Macedo, R.S.; Lima, R.d.C.C.; da Silva, M.V.; Pandorfi, H.; Silva, P.C.; de Oliveira-Júnior, J.F. Influence of Drought and Anthropogenic Pressures on Land Use and Land Cover Change in the Brazilian Semiarid Region. *J. S. Am. Earth Sci.* **2023**, *126*, 104362. [CrossRef]
5. Montenegro, A.A.d.A.; Abrantes, J.R.C.B.; de Lima, J.L.M.P.; Singh, V.P.; Santos, T.E.M. Impact of Mulching on Soil and Water Dynamics under Intermittent Simulated Rainfall. *Catena* **2013**, *109*, 139–149. [CrossRef]
6. Peña-Angulo, D.; Nadal-Romero, E.; González-Hidalgo, J.C.; Albaladejo, J.; Andreu, V.; Barhi, H.; Bernal, S.; Biddoccu, M.; Bienes, R.; Campo, J.; et al. Relationship of Weather Types on the Seasonal and Spatial Variability of Rainfall, Runoff, and Sediment Yield in the Western Mediterranean Basin. *Atmosphere* **2020**, *11*, 609. [CrossRef]
7. da Silva, M.V.; Pandorfi, H.; de Almeida, G.L.P.; de Lima, R.P.; dos Santos, A.; Jardim, A.M.d.R.F.; Rolim, M.M.; da Silva, J.L.B.; Batista, P.H.D.; da Silva, R.A.B.; et al. Spatio-Temporal Monitoring of Soil and Plant Indicators under Forage Cactus Cultivation by Geoprocessing in Brazilian Semi-Arid Region. *J. S. Am. Earth Sci.* **2021**, *107*, 103155. [CrossRef]
8. da Silva, M.V.; Pandorfi, H.; Lopes, P.M.O.; da Silva, J.L.B.; de Almeida, G.L.P.; Silva, D.A.d.O.; dos Santos, A.; Rodrigues, J.A.d.M.; Batista, P.H.D.; Jardim, A.M.d.R.F. Pilot Monitoring of Caatinga Spatial-Temporal Dynamics through the Action of Agriculture and Livestock in the Brazilian Semiarid. *Remote Sens. Appl. Soc. Environ.* **2020**, *19*, 100353. [CrossRef]
9. da Silva, J.L.B.; Moura, G.B.d.A.; da Silva, M.V.; Lopes, P.M.O.; Guedes, R.V.d.S.; e Silva, Ê.F.d.F.; Ortiz, P.F.S.; Rodrigues, J.A.d.M. Changes in the Water Resources, Soil Use and Spatial Dynamics of Caatinga Vegetation Cover over Semiarid Region of the Brazilian Northeast. *Remote Sens. Appl. Soc. Environ.* **2020**, *20*, 100372. [CrossRef]
10. Barbosa, H.A.; Kumar, T.V.L. Influence of Rainfall Variability on the Vegetation Dynamics over Northeastern Brazil. *J. Arid Environ.* **2016**, *124*, 377–387. [CrossRef]
11. Vieira, R.M.D.S.P.; Tomasella, J.; Barbosa, A.A.; Martins, M.A.; Rodriguez, D.A.; Rezende, F.S.D.; Carriello, F.; Santana, M.D.O. Desertification Risk Assessment in Northeast Brazil: Current Trends and Future Scenarios. *Land Degrad. Dev.* **2021**, *32*, 224–240. [CrossRef]
12. Bezerra, F.G.S.; Aguiar, A.P.D.; Alvalá, R.C.S.; Giarolla, A.; Bezerra, K.R.A.; Lima, P.V.P.S.; do Nascimento, F.R.; Arai, E. Analysis of Areas Undergoing Desertification, Using EVI2 Multi-Temporal Data Based on MODIS Imagery as Indicator. *Ecol. Indic.* **2020**, *117*, 106579. [CrossRef]
13. Moura, M.M.; Walter, L.S.; Lins, T.R.d.S.; Araujo, E.C.G.; da Cunha Neto, E.M.; Santana, G.M.; Brasil, I.D.S.; Silva, T.C. Temporal Analysis of Desertification Vulnerability in Northeast Brazil Using Google Earth Engine. *Trans. GIS* **2022**, *26*, 2041–2055. [CrossRef]

14. Vieira, R.M.d.S.P.; Sestini, M.F.; Tomasella, J.; Marchezini, V.; Pereira, G.R.; Barbosa, A.A.; Santos, F.C.; Rodriguez, D.A.; do Nascimento, F.R.; Santana, M.O.; et al. Characterizing Spatio-Temporal Patterns of Social Vulnerability to Droughts, Degradation and Desertification in the Brazilian Northeast. *Environ. Sustain. Indic.* **2020**, *5*, 100016. [CrossRef]
15. Albuquerque, P.I.D.M.; Rodrigues, J.P.B.; Peixoto, F.D.S.; Miranda, M.D.P. Sensoriamento Remoto Aplicado Em Indicadores de Desertificação No Municipio de Parelhas—RN. *Rev. Geogr.* **2020**, *37*, 241. [CrossRef]
16. da Silva, M.V.M.; Lima, C.E.S.; Silveira, C.d.S. Impact of Climate Change and Consumptive Demands on the Performance of São Francisco River Reservoirs, Brazil. *Climate* **2023**, *11*, 89. [CrossRef]
17. Melo, L.d.M.d.; Pessoa, M.M.d.L.; Silva, E.A.; Chaves, L.D.F.d.C. Landscape Change with the Transposition of the São Francisco River, in the Domain Caatinga, Pernambuco. *Floresta* **2021**, *51*, 648. [CrossRef]
18. Instituto de Pesquisa Econômica Aplicada (IPEA). *Transposição Do Rio São Francisco: Análise de Oportunidade Do Projeto*; IPEA: Rio de Janeiro, Brazil, 2011; ISBN 1415-4765.
19. Ministério do Desenvolvimento Regional (MDR). Projeto de Integração Do Rio São Francisco. Available online: https://www.gov.br/mdr/pt-br/assuntos/seguranca-hidrica/projeto-sao-francisco (accessed on 10 December 2022).
20. Silva, J.L.B.; Moura, G.B.A.; Silva, Ê.F.F.; Lopes, P.M.O.; Silva, T.T.F.; Lins, F.A.C.; Silva, D.A.O.; Ortiz, P.F.S. Spatial-Temporal Dynamics of the Caatinga Vegetation Cover by Remote Sensing in Municipality of the Brazilian Semi-Arid. *Rev. Bras. Ciências Agrárias—Braz. J. Agric. Sci.* **2019**, *14*, 1–10. [CrossRef]
21. Lins, F.A.C.; Araújo, D.C.D.S.; Da Silva, J.L.B.; Lopes, P.M.O.; Oliveira, J.D.A.; Gomes da Silva, A.T.C.S. Estimativa de Parâmetros Biofísicos e Evapotranspiração Real No Semiárido Pernambucano Utilizando Sensoriamento Remoto. *Irriga* **2017**, *1*, 64–75. [CrossRef]
22. Souza, C.M.; Shimbo, J.Z.; Rosa, M.R.; Parente, L.L.; Alencar, A.A.; Rudorff, B.F.T.; Hasenack, H.; Matsumoto, M.; Ferreira, L.G.; Souza-Filho, P.W.M.; et al. Reconstructing Three Decades of Land Use and Land Cover Changes in Brazilian Biomes with Landsat Archive and Earth Engine. *Remote Sens.* **2020**, *12*, 2735. [CrossRef]
23. Perez-Marin, A.M.; Cavalcante, A.M.B.; Medeiros, S.S.; Tinoco, L.B.M.; Salcedo, I.H. Núcleos de Desertificação No Semiárido Brasileiro: Ocorrência Natural Ou Antrópica? *Parcer. Estratégicas-CGEE* **2012**, *17*, 87–106.
24. Brito, P.V.D.S.; Morais, Y.C.B.; Ferreira, H.D.S.; da Silva, J.F.; Galvíncio, J.D. Análise Comparativa Da Umidade Da Vegetação de Áreas de Caatinga Preservada, Agricultura Irrigada e Sequeiro. *J. Environ. Anal. Prog.* **2017**, *2*, 493–498. [CrossRef]
25. Orusa, T.; Cammareri, D.; Borgogno Mondino, E. A Scalable Earth Observation Service to Map Land Cover in Geomorphological Complex Areas beyond the Dynamic World: An Application in Aosta Valley (NW Italy). *Appl. Sci.* **2022**, *13*, 390. [CrossRef]
26. Pielke, R.A.; Pitman, A.; Niyogi, D.; Mahmood, R.; McAlpine, C.; Hossain, F.; Goldewijk, K.K.; Nair, U.; Betts, R.; Fall, S.; et al. Land Use/Land Cover Changes and Climate: Modeling Analysis and Observational Evidence. *WIREs Clim. Chang.* **2011**, *2*, 828–850. [CrossRef]
27. Orusa, T.; Viani, A.; Cammareri, D.; Borgogno Mondino, E. A Google Earth Engine Algorithm to Map Phenological Metrics in Mountain Areas Worldwide with Landsat Collection and Sentinel-2. *Geomatics* **2023**, *3*, 221–238. [CrossRef]
28. Pielke, R.A. Land Use and Climate Change. *Science* **2005**, *310*, 1625–1626. [CrossRef] [PubMed]
29. de Oliveira-Júnior, J.F.; Shah, M.; Abbas, A.; Correia Filho, W.L.F.; da Silva Junior, C.A.; Santiago, D.d.B.; Teodoro, P.E.; Mendes, D.; de Souza, A.; Aviv-Sharon, E.; et al. Spatiotemporal Analysis of Fire Foci and Environmental Degradation in the Biomes of Northeastern Brazil. *Sustainability* **2022**, *14*, 6935. [CrossRef]
30. Pereira, J.D.A.; Cavalcanti, A.K.G.; Pires, A.L.; Rocha Neto, O.; Carvalho, J.V.A.; Santos, L.C.; Coelho, M.S.; Sousa, P.F.d.N. A Utilização de Sensoriamento Remoto Para Visualização de Possíveis Áreas Desertificadas Nos Municípios de Cajazeiras e Coremas, PB. *Braz. J. Dev.* **2020**, *6*, 18009–18021. [CrossRef]
31. Leonardo, H.R.D.A.L.; de Oliveira, L.M.M.; de Oliveira, E.F.; de Almeida, D.N.O.; de Paiva, A.L.R. Geotechnology in the Analysis of Behavior Spectral of Natural Resources in the Semiarid Pernambucano. *J. Hyperspectral Remote Sens.* **2019**, *9*, 191. [CrossRef]
32. Silva, J.R.I.; Montenegro, A.A.d.A.; Farias, C.W.L.d.A.; Jardim, A.M.d.R.F.; da Silva, T.G.F.; Montenegro, S.M.G.L. Morphometric Characterization and Land Use of the Pajeú River Basin in the Brazilian Semi-Arid Region. *J. S. Am. Earth Sci.* **2022**, *118*, 103939. [CrossRef]
33. Xu, H. Modification of Normalised Difference Water Index (NDWI) to Enhance Open Water Features in Remotely Sensed Imagery. *Int. J. Remote Sens.* **2006**, *27*, 3025–3033. [CrossRef]
34. da Silva, J.L.B.; Moura, G.B.d.A.; da Silva, M.V.; de Oliveira-Júnior, J.F.; Jardim, A.M.d.R.F.; Refati, D.C.; Lima, R.d.C.C.; de Carvalho, A.A.; Ferreira, M.B.; de Brito, J.I.B.; et al. Environmental Degradation of Vegetation Cover and Water Bodies in the Semiarid Region of the Brazilian Northeast via Cloud Geoprocessing Techniques Applied to Orbital Data. *J. S. Am. Earth Sci.* **2023**, *121*, 104164. [CrossRef]
35. da Silva, M.V.; Pandorfi, H.; de Oliveira-Júnior, J.F.; da Silva, J.L.B.; de Almeida, G.L.P.; Montenegro, A.A.d.A.; Mesquita, M.; Ferreira, M.B.; Santana, T.C.; Marinho, G.T.B.; et al. Remote Sensing Techniques via Google Earth Engine for Land Degradation Assessment in the Brazilian Semiarid Region, Brazil. *J. S. Am. Earth Sci.* **2022**, *120*, 104061. [CrossRef]
36. Companhia de Pesquisa de Recursos Minerais (CPRM). *Serviço Geológico Do Brasil. Projeto Cadastro de Fontes de Abastecimento Por Água Subterrânea: Diagnóstico Do Município de Cabrobó, Estado de Pernambuco*; CPRM: Sao Paulo, Brazil, 2005; Volume 22.
37. Companhia de Pesquisa de Recursos Minerais (CPRM). *Projeto Cadastro de Fontes de Abastecimento Por Água Subterrânea: Diagnóstico Do Município de Terra Nova, Estado de Pernambuco*; CPRM: Sao Paulo, Brazil, 2005; Volume 20.

38. Instituto Brasileiro de Geografia e Estatística (IBGE). Panorama Cabrobó. Available online: https://cidades.ibge.gov.br/brasil/pe/cabrobo/panorama (accessed on 5 December 2022).
39. Instituto Brasileiro de Geografia e Estatística (IBGE). Panorama Terra Nova. Available online: https://cidades.ibge.gov.br/brasil/pe/terra-nova/panorama (accessed on 5 December 2020).
40. Agência Pernambucana de Águas e Clima (APAC). O Projeto de Integração Do Rio São Francisco. Available online: https://www.apac.pe.gov.br/pisf (accessed on 1 June 2023).
41. Companhia de Desenvolvimento dos Vales do São Francisco e do Parnaíba (CODEVASF). Projeto São Francisco. Available online: https://www.codevasf.gov.br/linhas-de-negocio/projeto-sao-francisco/o-que-e-o-projeto-de-integracao-do-sao-francisco (accessed on 1 June 2023).
42. Alvares, C.A.; Stape, J.L.; Sentelhas, P.C.; Gonçalves, J.L.d.M.; Sparovek, G. Köppen's Climate Classification Map for Brazil. *Meteorol. Z.* **2013**, *22*, 711–728. [CrossRef] [PubMed]
43. Beck, H.E.; Zimmermann, N.E.; McVicar, T.R.; Vergopolan, N.; Berg, A.; Wood, E.F. Present and Future Köppen-Geiger Climate Classification Maps at 1-Km Resolution. *Sci. Data* **2018**, *5*, 180214. [CrossRef] [PubMed]
44. Instituto Nacional de Meteorologia (INMET). Normais Climatológicas. Available online: https://clima.inmet.gov.br/GraficosClimatologicos/ (accessed on 10 June 2022).
45. Soil Survey Staff. *Keys to Soil Taxonomy*, 9th ed.; US Department of Agriculture: Washington, DC, USA, 2006.
46. Agência Pernambucana de Águas e Clima (APAC). Ficha Técnica—Reservatório Nilo Coelho. Available online: http://200.238.107.184/images/media/1602286317_nilocoelhoFicha.pdf (accessed on 22 January 2023).
47. Agência Pernambucana de Águas e Clima (APAC). Relatório de Situação de Recursos Hídricos Do Estado de Pernambuco 2011/2012. Available online: https://www.lai.pe.gov.br/apac/wp-content (accessed on 16 June 2022).
48. United States Geological Survey (USGS). Earth Explorer. Available online: https://earthexplorer.usgs.gov/ (accessed on 1 December 2022).
49. Agência Pernambucana de Águas e Clima (APAC). Monitoramento Pluviométrico. Available online: http://old.apac.pe.gov.br/meteorologia/monitoramento-pluvio.php (accessed on 11 October 2022).
50. MapBiomas Brazil. Coleção 7.1 Da Série Anual de Mapas de Cobertura e Uso de Solo Do Brasil. Available online: https://mapbiomas.org/colecoes-mapbiomas-1?cama_set_language=pt-BR (accessed on 11 March 2023).
51. Rouse, J.W.; Haas, R.H.; Schell, J.A.; Deering, D.W.; Harlan, J.C. *Monitoring the Vernal Advancement of Retrogradation of Natural Vegetation*; NASA/GSFCT Type II Report; NASA: Washington, DC, USA, 1973.
52. Huete, A.R. A Soil-Adjusted Vegetation Index (SAVI). *Remote Sens. Environ.* **1988**, *25*, 295–309. [CrossRef]
53. Allen, R.G.; Tasumi, M.; Trezza, R. Surface Energy Balance Algorithm for Land (SEBAL)—Advanced Training and User's Manual. *Kimberly Ida. Implement.* **2002**, *1*, 98.
54. Ribeiro, R.B.; Filgueiras, R.; Ramos, M.C.A.; Nascimento, C.R. Análise Temporal Das Variações de Parâmetros Biofísicos Da Cana-de-Açúcar Em Jaíba—MG. *Nativa* **2015**, *3*, 150–155. [CrossRef]
55. Batista, P.H.D.; de Almeida, G.L.P.; da Silva, J.L.B.; Pandorfi, H.; da Silva, M.V.; da Silva, R.A.B.; de Melo, M.V.N.; Lins, F.A.C.; Cordeiro Junior, J.J.F. Short-Term Grazing and Its Impacts on Soil and Pasture Degradation. *Dyna* **2020**, *87*, 123–128. [CrossRef]
56. Barbosa, H.A.; Lakshmi Kumar, T.V.; Paredes, F.; Elliott, S.; Ayuga, J.G. Assessment of Caatinga Response to Drought Using Meteosat-SEVIRI Normalized Difference Vegetation Index (2008–2016). *ISPRS J. Photogramm. Remote Sens.* **2019**, *148*, 235–252. [CrossRef]
57. Tomasella, J.; Vieira, R.M.S.P.; Barbosa, A.A.; Rodriguez, D.A.; Santana, M.d.O.; Sestini, M.F. Desertification Trends in the Northeast of Brazil over the Period 2000–2016. *Int. J. Appl. Earth Obs. Geoinf.* **2018**, *73*, 197–206. [CrossRef]
58. Asner, G.P.; Scurlock, J.M.O.; Hicke, J.A. Global Synthesis of Leaf Area Index Observations: Implications for Ecological and Remote Sensing Studies. *Glob. Ecol. Biogeogr.* **2003**, *12*, 191–205. [CrossRef]
59. Kumar Nayan, N.; Das, A.; Mukerji, A.; Mazumder, T.; Bera, S. Spatio-Temporal Dynamics of Water Resources of Hyderabad Metropolitan Area and Its Relationship with Urbanization. *Land Use Policy* **2020**, *99*, 105010. [CrossRef]
60. Leite, P.A.M.; de Souza, E.S.; dos Santos, E.S.; Gomes, R.J.; Cantalice, J.R.; Wilcox, B.P. The Influence of Forest Regrowth on Soil Hydraulic Properties and Erosion in a Semiarid Region of Brazil. *Ecohydrology* **2018**, *11*, e1910. [CrossRef]
61. Singh, W.R.; Barman, S.; Tirkey, G. Morphometric Analysis and Watershed Prioritization in Relation to Soil Erosion in Dudhnai Watershed. *Appl. Water Sci.* **2021**, *11*, 151. [CrossRef]
62. Bi, L.; Fu, B.L.; Lou, P.Q.; Tang, T.Y. Delineation Water of Pearl River Basin Using Landsat Images from Google Earth Engine. *Int. Arch. Photogramm. Remote Sens. Spat. Inf. Sci.* **2020**, *XLII–3/W10*, 5–10. [CrossRef]
63. de Sousa, L.d.B.; Montenegro, A.A.d.A.; da Silva, T.G.F.; de Carvalho, A.A.; da Silva Neto, M.A. Estimativa Da Evapotranspiração Real e Mapeamento de Áreas Cultivadas Em Uma Bacia Do Projeto de Integração Do São Francisco (PISF), Semiárido Pernambucano. *Irriga* **2021**, *26*, 565–583. [CrossRef]
64. Bourke, S.A.; Shanafield, M.; Hedley, P.; Chapman, S.; Dogramaci, S. A Hydrological Framework for Persistent Pools along Non-Perennial Rivers. *Hydrol. Earth Syst. Sci.* **2023**, *27*, 809–836. [CrossRef]
65. De Carvalho Junior, A.P.; de Novais, R.P.; de Oliveira, M.A. A Perenização de Rios Através Da Construção de Açudes Para o Combate à Seca No Semiárido Nordestino. *Geopauta* **2022**, *6*, e9401. [CrossRef]

66. Lopes, A.V.; Dracup, J.A. The Sao Francisco Transboundary Project: Regulation and Sustainability. In Proceedings of the World Environmental and Water Resources Congress 2011, Palm Springs, CA, USA, 22–26 May 2011; American Society of Civil Engineers: Reston, VA, USA, 2011; pp. 2830–2839.
67. de Sousa, L.d.B.; Montenegro, A.A.d.A.; da Silva, M.V.; Almeida, T.A.B.; de Carvalho, A.A.; da Silva, T.G.F.; de Lima, J.L.M.P. Spatiotemporal Analysis of Rainfall and Droughts in a Semiarid Basin of Brazil: Land Use and Land Cover Dynamics. *Remote Sens.* **2023**, *15*, 2550. [CrossRef]

Disclaimer/Publisher's Note: The statements, opinions and data contained in all publications are solely those of the individual author(s) and contributor(s) and not of MDPI and/or the editor(s). MDPI and/or the editor(s) disclaim responsibility for any injury to people or property resulting from any ideas, methods, instructions or products referred to in the content.